5-2019

Modeling and Validation of Tissue Optical Properties in the Photon Transport Regime

Katelyn Heath

Modeling and Validation of Tissue Optical Properties in the Photon Transport Regime

An Undergraduate Honors College Thesis

in the Department of Biomedical Engineering College of Engineering University of Arkansas Fayetteville, AR

By Katelyn Heath

Table of Contents

1. Abstract

Early detection of changes in epithelial cells, such as the development of neoplastic formations seen in epithelial dysplasia, can indicate regions of the epithelial tissue that are at a high risk for cancerous formation. Using concepts from diffuse reflectance spectroscopy, a Monte Carlo model was developed to predict the reflectance measured by a detector at a small source-detector separation on a microendoscope. The Monte Carlo results were then used to calculate a mathematical relationship between the reflectance and distance that can be used to determine optical properties in a tissue sample. This model was validated with liquid phantoms of specified optical properties. The model was able to create a reflectance map based on specified optical properties. It was not, however, able to correctly predict the relationship between reflectance and distance for the phantoms that were tested. Improvements to the model, such as adding cladding element to the laser to change its numerical aperture, will continue to improve its accuracy.

2. Introduction

Early detection of changes in epithelial cells, such as the development of neoplastic formations seen in epithelial dysplasia, can indicate regions of the epithelial tissue that are at a high risk for cancerous formation. [1] Dysplasia can arise in the gastrointestinal tract and upper aerodigestive tract, as well as other locations with epithelial cells. [1-2] The current method of assessing for epithelial dysplasia requires biopsy of the tissue and assessing the cells with a microscope for changes the cells. This method can prove challenging as dysplastic cells can be difficult to distinguish from normally regenerating cells. A method of easily distinguishing between these cell types would hugely improve diagnosis for dysplasia. [2]

Diffuse Reflectance Spectroscopy has been shown to quantify functional information about tissue at short depths, such as the surface of the epithelium [3]. In this method, light is sent into tissue where it undergoes scattering and absorption phenomenon. Some of that light scatters to the point that it reverses direction back towards the surface of the tissue, so that it has been reflected, as seen in **Figure 1.** A detector is placed a short distance away from the illumination fiber. This distance is very small, often on the 10^-6 scale, as light in unable to penetrate far into tissue before it is absorbed completely. The information collected by the detector can then be used to relate the intensity of reflectance in the tissue to its optical properties with an inverse model. [4] **It** has been shown to have the potential to be applied in clinic for the diagnosis of malignancy in cells. [3] Its non-invasiveness and low subjectivity makes it a favorable option as a diagnostic tool. [4]

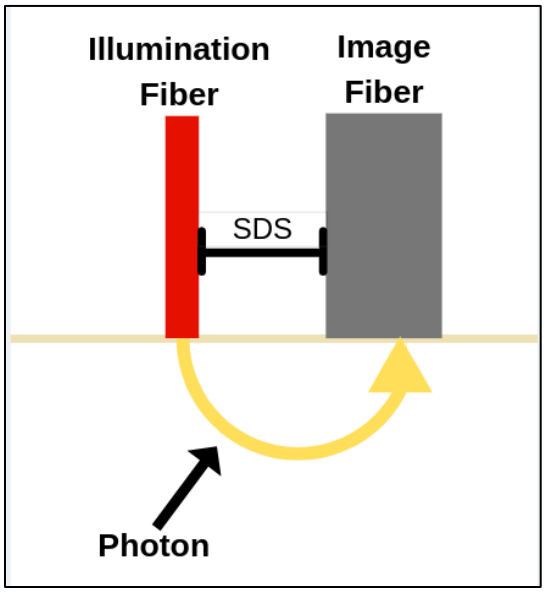

Figure 1. The setup Diffuse Reflectance Spectroscopy (DRS). The source-detector separation (SDS) is seen as the distance between the illumination fiber and image fiber. A photon is sent into the tissue from the illumination fiber, backscatters in the tissue and is reflected back to the image fiber where it is stored in an image.

Using concepts from diffuse reflectance spectroscopy, a Monte Carlo model will be developed to predict the reflectance measured by a detector at a small source-detector separation on a microendoscope. The Monte Carlo results will then be used to calculate a mathematical relationship between the reflectance and distance that can be used to determine optical properties in a tissue sample. This model will be validated with liquid phantoms of specified optical properties.

3. Materials

3.1 TracePro and Monte Carlo Modeling

TracePro (Lambda Research Corporation) is a digital tool that combines CAD with Monte Carlo ray tracing. Monte Carlo is a statistical method that approximates a chain of events based on some parameter, such as scattering and absorption. The path of each of each photon is traced throughout the tissue, with the probability of scattering and absorption events occurring over a unit distance. This is specified by the user as scattering and absorption coefficients of the tissue. These parameters are independent of each other and characteristics of the tissue type. The simulation returns spatial information about the photons. [5]

3.2 Phantoms

Phantoms were composed of blue food dye (McCormick & Company, USA) for the absorbing agent, 1 μm-diameter polystyrene microspheres (07310-15, Polysciences, USA) for the scattering component, and deionized water. The absorption spectrum for a stock food dye solution containing 150 mL of DI water mixed with 1 mL of food dye was taken using a spectrophotometer from 400-900 nm. Using the absorption value found at 633 nm and the known scattering value of the

microspheres at this wavelength, a recipe was formulated. Mie Theory was used to create liquid samples with predictable optical properties, as seen in **Figure 2**. [6]

	μa' (1/cm)	μa' (1/cm)
Phantom 1	2.904	1.987
Phantom 2	2.904	10.93

Figure 2. Absorption and Scattering coefficients of each phantom at 633 nm.

3.3 Instrumentation

The microendoscope (Myriad Fiber Imaging, USA) used for this experiment is a fiber optic probe consisting of a combination of five 220 μm multi-modal fibers surrounding a 1 mm image fiber. The central imaging fiber is composed of 50,000 individual fiber elements. This fiber is surrounded by a 0.1 mm ring that can be seen in the images but was removed from all computation. The distance from the center of each 220 μm fiber and the image fiber is 845 μm. The full length of the fiber-optic probe is 4 ft. **Figure 3** shows the details of the fiber-optic probe [6[. The first fiber and the image fiber were used for imaging the phantoms.

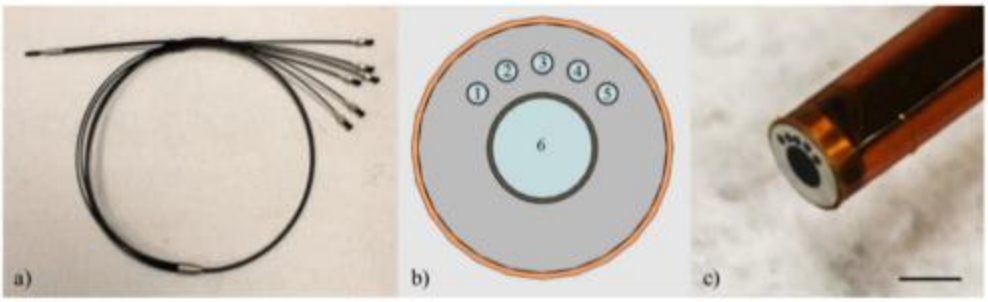

Figure 3. Microendoscope used for data collection. a) A full view of the 4ft. long fiber. b) A cross section view of the fiber tip. The central image fiber is surrounded by five smaller fibers. c) A side view of the tip of the device. [6]

4. Methods

4.1 TracePro Simulation

The simulation, created in TracePro, was produced using its CAD capabilities with the same dimensions as the image and illumination fibers and the liquid phantoms, as seen in **Figure 4**. The simulation traced 10^8 photons from the source, representing the 633 nm laser, through the tissue. Some of these photons backscattered, coming into contact with the detector. Information about the photons that came into contact with the detector was stored, such as the position they encountered the detector and their incident vector. For phantom 1, about 1.6*10^6 photons encountered the detector, while for phantom 2, about 7*10^6.

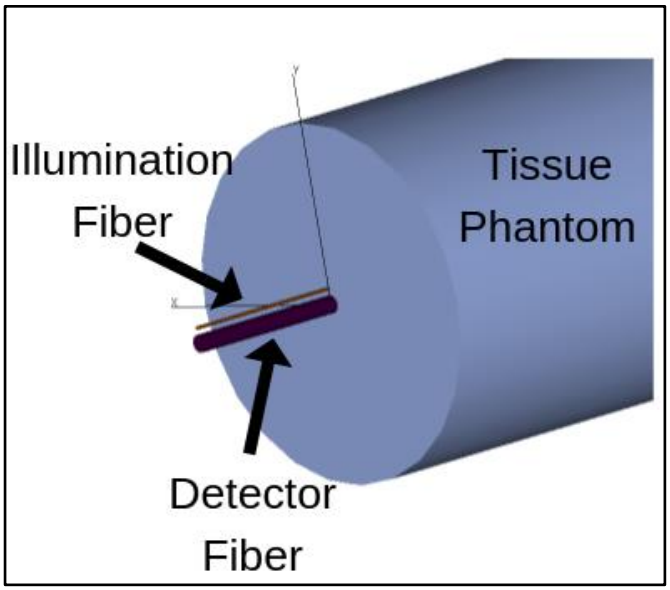

Figure 4. Image of the TracePro Simulation. The illumination fiber, detector fiber, and phantom are shown.

Using the information from the simulation, a map of the density of incident photons was created. Using their incident vector information, photons that were incident at an angle that was greater than the numerical aperture (NA) of the endoscope were removed, as they would not have been detected. The angle was found using the equation for NA, NA=n*sin(theta), where n is the index of refraction and theta is the half-angle of the night that can enter the lens. This can be seen in **Figure 5**. The photon map was then segmented into bins 10 μm in length and diameter. The value of each bin refers to the number of photons that were incident in that space. The bins along the center, horizontal direction away from the illumination fiber were isolated. The value of these bins, or the quantity of incident photons, was plotted against the source detector separation from the center of each bin. This plot was then fitted to a power law equation (y=ax^b+c) using the Matlab curve fitting tool.

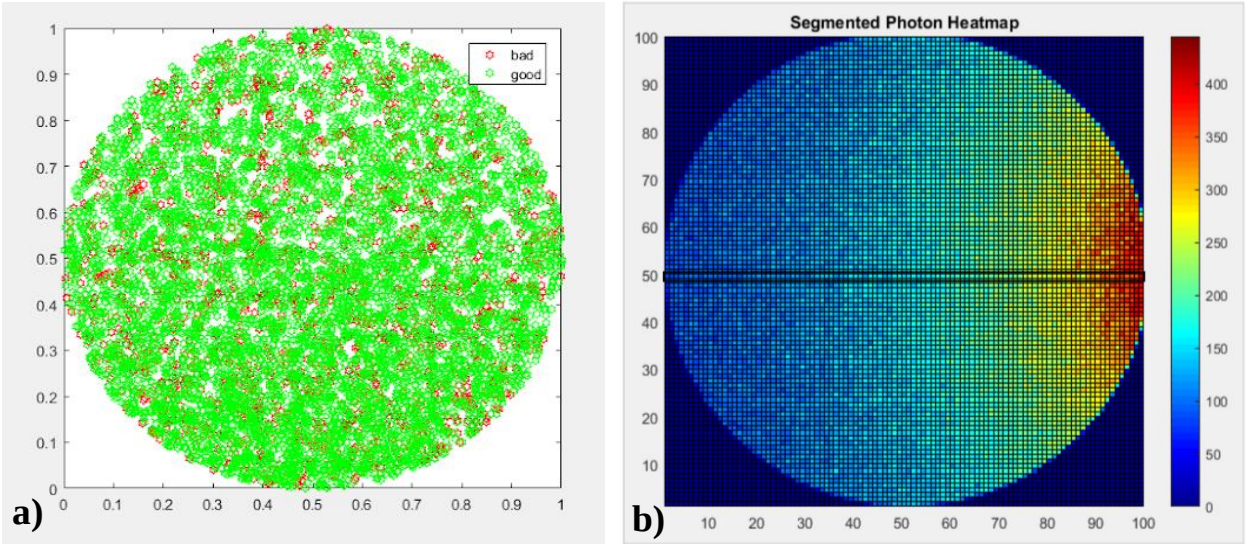

Figure 5. a) Image of detector surface with incident photons marked. Photons within NA marked in green, photos out of NA in red. b) Image of Segmented Photon Heatmap, with the center horizontal line marked.

4.2 Phantom Imaging

Images of liquid phantoms were then taken to validate the ability of the simulation to create a reflectance curve based on specific optical properties, as seen in **Figure 6**. A 633 nm laser was sent through the first 220 μm fiber and into the phantom. A camera connected to the central image fiber took images with a 1450 ms integration time. This was the highest integration time that could be used without either image becoming saturated. The images were segmented into 100 square bins and the intensity of each pixel in that bin was summed. The source-detector separation was plotted against the reflectance intensity of each bin and fitted to power law using the Matlab curve fitting tool.

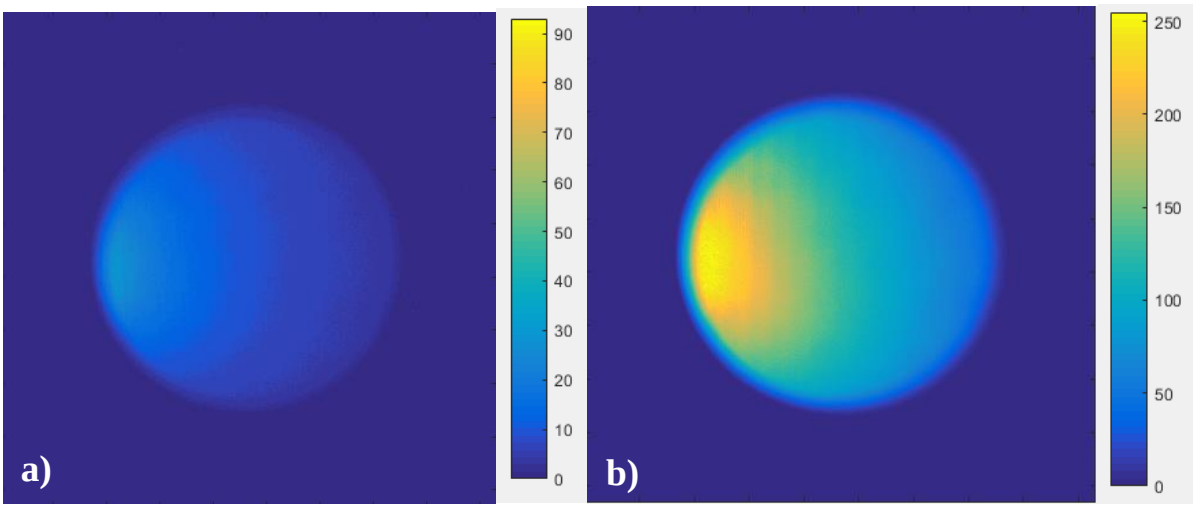

Figure 6. Images of the phantoms taken with the microendoscope. The color bar refers to the reflectance value at each pixel. a) Refers to Phantom 1. b) Refers to Phantom 2.

5. Results

The model was able to create a reflectance map based on specified properties as seen in **Figure 7**. It was not, however, able to correctly predict the relationship between reflectance and distance for the phantoms that were tested. In order for our model to be validated, the simulated curve would be equivalent to the measured curve. In both cases, the exponential coefficient (B) was greater in the experiment that in the simulation. For the phantom with the greater scattering coefficient of 10.93 [1/cm] (Phantom 2), the exponential coefficient (B) for the simulation was an order of magnitude less than that of the experimental data.

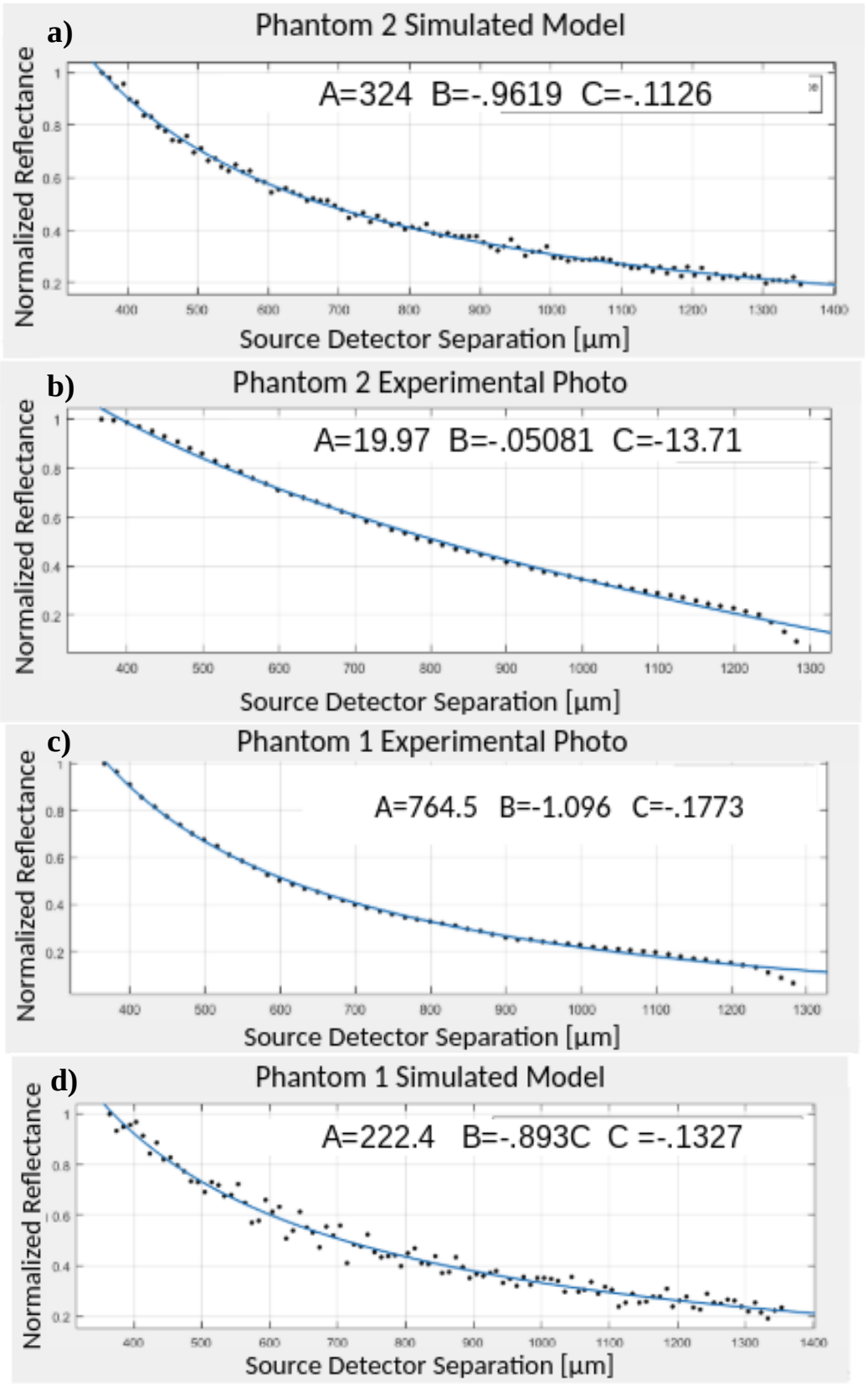

Figure 7. Plots of the Source Detector Separation vs. Normalized Reflectance. a) and c) are for the simulated phantoms. b) and d) are for the experimentally measured phantoms.

6. Discussion

The model was unable to be verified by the experimental data. The differences between the simulations and the experiments were most likely due to an unconsidered parameter of the model. One possible solution that I propose is that the numerical aperture of the illumination beam was not included in the model. Because of the small magnitude of the fiber, the light exiting the illumination fiber could be modeled as a conical ray instead of a completely perpendicular one as is considered in this model.

7. Future Work

Improvements to the model, such as adding cladding element to the laser to change its numerical aperture, will continue to improve its accuracy. Multi-layer phantoms that better simulate the epithelium could be used to better verify the models ability to work in more complicated morphologies.

8. Acknowledgements

I would like to thank Gage Greening for assistance in building my phantoms and Dr. Muldoon for his wonderful mentorship. This work was supported by the National Science Foundation (CBET 1751554) and the Arkansas Biosciences Institute.

References

[1] Sharma, P., & Montgomery, E. (2013). Gastrointestinal dysplasia. Pathology, 45(3), 273-285. doi:10.1097/pat.0b013e32835f21d7

[2] Speight, Paul M. “Update on Oral Epithelial Dysplasia and Progression to Cancer.” Head and Neck Pathology, vol. 1, no. 1, Sept. 2007, pp. 61–66., doi:10.1007/s12105-007-0014-5.

[3] Jayanthi, J. L., et al. “Diffuse Reflectance Spectroscopy: Diagnostic Accuracy of a Non-Invasive Screening Technique for Early Detection of Malignant Changes in the Oral Cavity.” BMJ Open, vol. 1, no. 1, 24 June 2011, doi:10.1136/bmjopen-2011-000071.

[4] Hennessy, Ricky, et al. “Effect of Probe Geometry and Optical Properties on the Sampling Depth for Diffuse Reflectance Spectroscopy.” Journal of Biomedical Optics, vol. 19, no. 10, 27 Oct. 2014, p. 107002., doi:10.1117/1.jbo.19.10.107002.

[5]Kanick, S., Robinson, D., Sterenborg, H., & Amelink, A. (2010). Monte Carlo Analysis of Single Fiber Reflectance Path Length and Sampling Depth. Biomedical Optics and 3-D Imaging, 54(22), 6991-7008. doi:10.1364/biomed.2010.bsud40

[6] Greening, G. J., James, H. M., Powless, A. J., Hutcheson, J. A., Dierks, M. K., Rajaram, N., & Muldoon, T. J. (2015). Fiber-bundle microendoscopy with sub-diffuse reflectance spectroscopy and intensity mapping for multimodal optical biopsy of stratified epithelium. Biomedical Optics Express, 6(12), 4934. doi:10.1364/boe.6.004934